# Human BST-2/Tetherin inhibits Junin virus release from host cells and its inhibition is partially counteracted by viral nucleoprotein

Vahid Rajabali Zadeh[1,2], Shuzo Urata[1,3], Miako Sakaguchi[4], and Jiro Yasuda[1,2,3*]

[1] Department of Emerging Infectious Diseases, Institute of Tropical Medicine (NEKKEN), Nagasaki University, Nagasaki, Japan.

[2] Program for Nurturing Global Leaders in Tropical and Emerging Communicable Diseases, Graduate School of Biomedical Sciences, Nagasaki University, Nagasaki, Japan.

[3] National Research Center for the Control and Prevention of Infectious Diseases (CCPID), Nagasaki University, Nagasaki, Japan.

[4] Central Laboratory, Institute of Tropical Medicine (NEKKEN), Nagasaki University, Nagasaki, Japan.

*Corresponding author: Jiro Yasuda, j-yasuda@nagasaki-u.ac.jp

**KEY WORDS**

Junin virus, *Arenaviridae*, human BST-2, innate immunity, Tetherin

**ABBREVIATIONS:** BST-2, Bone marrow stromal cell antigen-2; JUNV, Junin virus; VLP, virus-like particle; IFN, interferon; ISG, interferon-stimulated gene; LCMV, lymphocytic choriomeningitis virus; MACV, Machupo virus; VSV, Vesicular stomatitis virus.

## ABSTRACT

Bone marrow stromal cell antigen-2 (BST-2), also known as Tetherin, is an interferon-inducible membrane-associated protein. It effectively targets enveloped viruses at the release step of progeny viruses from host cells, thereby restricting the further spread of viral infection. Junin virus (JUNV) is a member of *Arenaviridae,* which causes Argentine hemorrhagic fever that is associated with a high rate of mortality. In this study, we examined the effect of human BST-2 on the replication and propagation of JUNV. The production of JUNV Z-mediated virus-like particles (VLPs) was significantly inhibited by over-expression of BST-2. Electron microscopy analysis revealed that BST-2 functions by forming a physical link that directly retains VLPs on the cell surface. Infection using JUNV showed that infectious JUNV production was moderately inhibited by endogenous or exogenous BST-2. We also observed that JUNV infection triggers an intense interferon response, causing an upregulation of BST-2, in infected cells. However, the expression of cell surface BST-2 was reduced upon infection. Furthermore, the expression of JUNV nucleoprotein (NP) partially recovered VLP production from BST-2 restriction, suggesting that the NP functions as an antagonist against antiviral effect of BST-2. We further showed that JUNV NP also rescued the production of Ebola virus VP40-mediated VLP from BST-2 restriction as a broad spectrum BST-2 antagonist. To our knowledge, this is the first report showing that an arenavirus protein counteracts the antiviral function of BST-2.

## INTRODUCTION

Junin virus (JUNV) belongs to the genus *Mammarenavirus* of the family *Arenaviridae*, and is a causative agent of Argentine hemorrhagic fever (AHF) with severe clinical manifestations, including hemorrhage, thrombocytopenia, and neurological symptoms, and a 15 to 30 % case fatality. The disease is endemic to central Argentina, with more than 5 million people at risk of infection (1,2). Current countermeasures against AHF are limited to the live attenuated vaccine, Candid #1, which is only licensed in Argentina. Owing to the potential aerosol transmission, severe clinical manifestations, and a lack of FDA-approved vaccines/drugs, JUNV is classified as a category A bioterrorism agent. According to the National Institute of Allergy and Infectious Diseases, JUNV is a priority pathogen for defense programs, along with six other members of *Arenaviridae*, including Lassa virus (LASV). These facts emphasize the need to develop new treatment and immunization strategies against JUNV infections (3,4).

The viruses belonging to the genus *Mammarenavirus* are pleomorphic, enveloped viruses with size ranging from 40 to 200 nm. The virus genome is composed of two segments of ambisense RNA, the L segment (~7,200 nucleotides (nt)), which encodes the viral matrix protein Z and RNA-dependent RNA polymerase (L), and the S segment (~3,400 nt), which encodes the surface glycoprotein precursor (GPC) and nucleoprotein (NP) (5,6). The Z protein is known to play a central role in virus particle formation and budding. In fact, the sole expression of the Z protein is sufficient to produce virus-like particles (VLPs) (7–9). It is also reported that Z protein regulates viral gene expression and replication (10). The GPC is co- and post-translationally processed into the stable signal peptide (SSP), GP1 and GP2 subunits. GP1 is responsible for the recognition of the transferrin receptor 1 on the host cell membrane (11). Following a successful attachment to the host cell surface, the JUNV is internalized via a clathrin-mediated endocytosis pathway into a late endosome, wherein GP2 mediates the fusion of viral and cell membrane in low pH. Upon the release of viral ribonucleoprotein complex

into the cytoplasm, the L protein begins the transcription and replication of the viral genome together with the NP; as a result, dsRNA molecules are formed. Cytoplasmic RNA sensors, such as retinoic acid-inducible gene I (RIG-I), recognize these non-self RNAs and mount an interferon (IFN)-mediated, non-specific immune response to JUNV infection (12).

Bone marrow stromal cell antigen-2 (BST-2, also known as Tetherin, CD317, and HM1.24) is an IFN-stimulated gene (ISG) with a broad antiviral spectrum against enveloped viruses (13–17). One of the major antiviral mechanisms of BST-2 is prevention of the release of progeny virions from host cells and tethering them onto the cell surface (18–20). BST-2 is a type II transmembrane protein with an N-terminal cytoplasmic domain, a coiled-coil extracellular domain (containing two N-linked glycosylation residues), and a C-terminal glycosylphosphatidylinositol (GPI) anchor. The protein can also form homodimers by the interaction of cysteine residues of the ectodomain (21,22). Studies have shown that the transmembrane domain along with the GPI anchor is essential for the function of BST-2 as a viral restriction factor (23). However, it has been argued whether the dimerization of BST-2 is essential for its antiviral activity (24). The antiviral activity of BST-2 was first reported in human immunodeficiency virus (HIV)-1 (25). Subsequently, it was demonstrated that BST-2 also inhibits the egress of VLPs of several other enveloped viruses including filoviruses (Ebola and Marburg viruses) and arenaviruses (LASV, lymphocytic choriomeningitis virus (LCMV), and Machupo virus (MACV)) (26). Furthermore, the experiments using the prototype arenavirus, LCMV, and LASV provided evidence that BST-2 can also restrict the propagation of the infectious progeny of arenaviruses (13,26,27). However, it remains unclear whether BST-2 has a similar function against JUNV.

Some viruses have evolved and acquired mechanisms to antagonize the antiviral activity of BST-2. The HIV-1 accessory protein Vpu is a well-characterized BST-2 antagonist, which ubiquitinates BST-2 and down-regulates BST-2 expression through proteasome-dependent

91 degradation (28–31). In contrast, the Ebola virus (EBOV) glycoprotein (GP) is known to
92 antagonize BST-2 by a direct physical interaction, without the need for cell surface BST-2
93 down-regulation or degradation. The HIV-2 envelope glycoprotein Env, influenza virus M2
94 protein, and Kaposi's sarcoma herpesvirus K5/MIR2 are among other recognized BST-2
95 antagonists (32–36).

96 In this study, we investigated the antiviral activity of BST-2 against JUNV replication and
97 propagation. Our results showed that BST-2 restricts JUNV Z-mediated VLP production, while
98 the reduction of JUNV production by BST-2 is modest. We found that the cell surface
99 expression of BST-2 is reduced by JUNV infection, although JUNV infection induces IFN
100 response and sequential BST-2 expression, and that the antiviral action of BST-2 against JUNV
101 is partially antagonized by NP. This is the first report that the NP of JUNV enables the rescue
102 of VLPs by counteracting the antiviral action of human BST-2 protein.

103

## MATERIALS AND METHODS

**Cells, plasmids, and viruses.** 293T (Human embryonic kidney), HeLa (human cervix), A549 (human alveolar adenocarcinoma), and Vero 76 (African green monkey kidney) cell lines were maintained in Dulbecco's modified Eagle's medium (DMEM; Invitrogen, Carlsbad, CA, USA) containing 10 % fetal bovine serum (FBS) and 1 % penicillin and streptomycin (37). The generation of HeLa-pLKO (control HeLa cells) and HeLa-TKD (stable siRNA-mediated BST-2 knocked-down HeLa cells) was previously described (27). Constructions of the expression plasmids for human BST-2 (pCDNFL-hTeth), EBOV GP (pCEboZ-GP) and VP40 (pCEboZVP40) have also been described previously (13,38,39). To generate pC-JUNV-Z-FLAG plasmid, the cDNA coding for the Candid #1 Z gene was amplified by RT-PCR, and inserted into a pCAGGS plasmid containing the FLAG tag at the C-terminal. Plasmids expressing JUNV NP (pC-Candid-NP), GPC (pC-JUNV-GPC) and L (pC-Candid -L) proteins as well as Candid #1 vaccine strain of JUNV were kindly provided by Dr. J. C. de la Torre (The Scripps research Institute, California, USA) (40). A modified version of pC-Candid-NP with a FLAG tag at C-terminal (pC-Candid-NP-FLAG) was constructed using KOD Plus mutagenesis kit (TOYOBO, Osaka, Japan) using two primers (sense 5'-GACGATGACGACAAGTAAGCAGTGGGAGAGACGATTCTAG-3' and antisense 5'-TTTGTAGTCACCACCCAGTGCATAGGCTGCCTTCGGGAGG-3'). Vesicular stomatitis Indiana virus (VSV) was prepared as previously described (41).

**Virus infection and titration.** For virus infection, the cells were infected at an MOI = 0.1, 1, or 5, and allowed for adsorption at 37 ℃, for 1 h. The inoculum was then removed, washed with PBS (-), fresh DMEM was added to the monolayer, and incubated at 37 ℃ in the presence of 5 % $CO_2$. In order to measure the viral titers, plaque assay was performed according to the

standard procedures using 10-fold dilutions of samples in Vero 76 cell lines as described previously for LCMV titration (27).

**VLP assay.** Trans-IT LT-1 (Mirus BIO, Madison, WI, USA) or Lipofectamine 3000 (Invitrogen, Carlsbad, CA, USA) was used to transfect pC-JUNV-Z-FLAG plasmids alone or in combination with other plasmids in 293T and HeLa cells respectively. At 24 or 48 h post transfection (p.t.), the culture supernatants containing VLPs were briefly clarified from debris by centrifugation (1500 × *g* for 5 min at 4 °C). Ultra-centrifugation (195,000 × *g* for 30 min at 4 °C) was performed over a 20 % sucrose cushion to sediment VLPs. Pellets were re-suspended in PBS (-) and lysed in sodium dodecyl sulfate (SDS) lysis buffer (1 % NP-40, 50 mM Tris-HCl [pH 8.0], 62.5 mM EDTA, and 0.4 % sodium deoxycholate). The prepared samples were analyzed by SDS polyacrylamide gel electrophoresis (SDS-PAGE) and western blotting (WB). EBOV VP40 samples were prepared as previously described (42).

**Western blotting (WB).** The samples were separated using SDS-PAGE, and transferred onto a nitrocellulose membrane (10600016, Amersham, Munich, Germany). The membranes were then blocked using 5 % skim milk for 1 h at room temperature (RT). For the detection of FLAG-tagged Z/BST-2 proteins, membranes were incubated with mouse monoclonal anti-FLAG antibodies (M2, F1804, Sigma, St. Louis, MO, USA). For the detection of endogenous BST-2 and β-Actin, anti-human BST-2 polyclonal antibody produced in rabbit (provided from NIH AIDS Reagent Program; Catalog number 11721; received from Drs. Klaus Strebel and Amy Andrew) and anti-β-Actin monoclonal antibody produced in mouse (A1978, Sigma, St. Louis, MO, USA) were used, respectively. The antigen-antibody complexes were then labelled with HRP-conjugated anti-rabbit IgG antibody (W401B, Promega, Madison, WI, USA) or HRP-

conjugated anti-mouse IgG antibody (A2304, Sigma, St. Louis, MO, USA). The detection of EBOV VP40 and GP was described previously (38). The labelled proteins were then visualized by ECL prime (RPN2236, GE Healthcare) and LAS3000 (GE Healthcare), according to the manufacturer's instructions. The results were quantified using Multi Gauge software (Fuji Film, Tokyo, Japan).

**Transmission Electron Microscopy (TEM).** For electron microscopy, 293T cells were transfected with control plasmid or pC-JUNV-Z-FLAG with or without pCDNFL-hTeth. At 24 h p.t., cells were fixed in 2 % glutaraldehyde (Nacalai Tesque, Kyoto, Japan) in 0.1 M sodium cacodylate buffer containing 1 mM $CaCl_2$ and 1 mM $MgCl_2$ (cacodylate buffer, pH 7.4), at 4 °C for 60 min. The samples were rinsed with cacodylate buffer and then post-fixed with 1 % $OsO_4$ (Nacalai Tesque) in cacodylate buffer at 4 °C for 60 min. They were then washed with cacodylate buffer, dehydrated in a graded series of ethanol and acetone, and embedded in Quetol 651 epoxy resin (Nisshin EM, Tokyo, Japan). The resin-embedded samples were trimmed and sectioned using a diamond knife on an ultra-microtome (Reichert-Jung, Austria). Ultra-thin sections were collected on grids, and stained with uranyl acetate and lead citrate. The samples were examined at 80 kV under TEM (JEM-1230; JEOL, Tokyo, Japan).

**Quantification of human *Ifn-β* mRNA.** PCR primers targeting the mRNA sequence of human *Ifn-β* (sense 5′-TCTCCTGTTGTGCTTCTCCAC-3′, antisense 5′-GGCAGTATTCAAGCCTCCCA-3′) and glyceraldehyde-3-phosphate dehydrogenase (*Gapdh*) housekeeping gene (sense 5′-CAAATTCCATGGCACCGTCA-3′, antisense 5′-TAGTTGCCTCCCCAAAGCAC-3′), were designed using NCBI/primer BLAST. Total RNA from mock and infected cells were extracted using the RNeasy Mini Kit (74106, QIAGEN,

Hilden, Germany), following the manufacturer's instructions. DNase treatment was performed to ensure the removal of genomic contaminants (2270A, Takara, Shiga, Japan). Further, cDNA synthesis and PCR amplification were performed using a One Step TB Green PrimeScript Plus RT-PCR kit (RR096A, Takara, Shiga, Japan) using an ABI 7500 thermocycler (Applied Bio systems, Foster City, CA, USA), with the following reaction conditions: 42 ℃ for 5 min, 95 ℃ for 5 sec, and 60 ℃ for 34 sec, for a total of 35 cycles. Relative fold-change in expression levels was determined by the ΔΔCt calculation for quantitative real time PCR data.

**Quantification of bioactive human IFN-β.** The bioactive IFN-β in cell culture supernatant was measured based on the fact that elevating concentrations of IFN can protect against the cytopathic effect of VSV in Vero 76 cell lines (43). Supernatant from mock and JUNV (Candid #1)-infected HeLa cells at 12, 24, and 48 h p.i. was collected and exposed to UV for 5 min to inactivate infectious particles. Subsequently, the UV-treated supernatant was added to the Vero 76 cells for overnight incubation at 37 ℃, in the presence of 5 % $CO_2$. Inactivation of the virus was confirmed by performing the plaque assay. The following day, Vero 76 cells were washed with PBS (-) and inoculated with VSV at an MOI = 0.01 for 30 min adsorption time. Culture media was added to the wells after the viruses were washed out with PBS (-). The cells were incubated for another 6 h. The VSV titers from mock and JUNV (Candid #1)-infected samples were compared. Recombinant IFN-β (300-02B, PEPRotech, NJ, USA) of 10, 100, and 1000 international units (IU)/ml were used as controls (data not shown).

**Fluorescence-activated cell sorting (FACS) analysis.** Cells were washed with PBS (-), detached using Accutase (AT104; Innovative cell technologies, INC., San Diego, CA, USA), and then collected in PBS (-). Subsequently, fixation was performed using 2%

paraformaldehyde (PFA) for 10 min at RT. Cells were then washed and re-suspended with PBS (-) containing 10 % FBS for blocking, and incubated at 4 ℃ for 30 min. For staining of intracellular BST-2, permeabilization reagent containing 0.3 % Triton X-100 was added to the 10 % FBS blocking buffer. Cells were then divided into two tubes for the PE-conjugated mouse monoclonal control antibody (MOPC-21; Biolegend, San Diego, CA, USA) or PE-conjugated mouse monoclonal anti-human-BST-2 antibody (RS38E; Biolegend) and stained for 5 h, at 4 ℃. Fluorescent signals were acquired using a flow cytometer (FACS Caliber, BD Bio sciences, San Jose, CA, USA). Data were analyzed using FlowJo software (Tree Star, version 10.0.7).

**Immunofluorescence analysis.** A549 cells were transfected with 0.5 μg of pC-JUNV-NP-FLAG plasmid. At 24 h p.t., cells were treated with 1000 IU/ml of IFN-β (300-02B, PEPRotech, NJ, USA). After overnight incubation, cells were re-seeded in millicell EZ slide (PEZGS0816, (Merck Millipore, Darmstadt, Germany). Once attached, cells were then fixed with 4 % paraformaldehyde. Permeabilization was performed using 0.3 % Triton X-100 in PBS containing 3 % BSA. Cells were incubated with rabbit polyclonal anti-FLAG antibody (F7245, Sigma, St. Louis, MO, USA) for overnight at 4 ℃ and then the incubation was followed by anti-rabbit IgG-FITC (ab6009, Abcam, Cambridge, UK) and PE-conjugated mouse monoclonal anti-human-BST-2 antibody (RS38E; Biolegend, San Diego, CA, USA). DAPI was used to stain nuclei. Samples were examined by the laser confocal microscopy (LSM780; Carl Zeiss, Oberkochen, Germany).

**Statistical analysis.** Student's t-test was used to determine the statistically significant differences in the mean values among test and control groups (not significant, [NS]; $p < 0.05$, *; $p < 0.01$, **).

## RESULTS

### BST-2 inhibits JUNV Z-mediated VLP production

To investigate if BST-2 restricts JUNV Z-mediated VLP production, we employed a previously described (5) and widely used VLP assay. The 293T cells, which do not express BST-2 endogenously (29), were co-transfected with the expression plasmids for FLAG-tagged JUNV Z and FLAG-tagged BST-2. The VLPs were collected from the culture supernatant at 24 h p.t. by ultracentrifugation. Cell lysates were prepared as described in the materials and methods. Expression of VLP-associated and intracellular Z protein as well as BST-2 was assessed by western blotting (WB), using an antibody against FLAG-tag. Levels of β-Actin were examined as the loading control. Even though the intracellular expression levels of Z protein remained unchanged, VLP production was significantly reduced (93.5 %) upon BST-2 expression (Fig. 1A and B). Furthermore, transmission electron microscopy (TEM) analysis revealed retention and clustering of VLPs on the plasma membrane in presence of BST-2 as compared to the 293T cells which expressed only JUNV Z protein (Fig. 1C), as we previously observed with LASV Z protein (13).

### BST-2 moderately restricts JUNV multiplication

To extend our observation that BST-2 inhibits JUNV Z-mediated VLP production, the infectious vaccine strain of JUNV (Candid #1) was used, which can be handled at a Biosafety Level-2 laboratory. The HeLa cell line is known to express high levels of BST-2 endogenously (44). The BST-2 knocked-down HeLa cell line (HeLa-TKD) and control cell line (HeLa-pLKO) were established as described previously (27). The knock-down of BST-2 expression in HeLa-TKD was confirmed by WB analysis using an anti-BST-2 antibody (Fig. 2A). To examine the effect of BST-2 on virus replication and propagation, both the cell lines were

infected with JUNV (Candid #1), at a multiplicity of infection (MOI) of 0.1. Virus-containing media was replaced with fresh media at 1 hour post infection (h p.i.), and culture supernatant was collected at 24 and 48 h p.i.. A modest increase in JUNV production was observed in HeLa-TKD cells compared to HeLa-pLKO cells at 24 and 48 h p.i. (1.95 and 1.87 times, respectively) (Fig. 2B). We next examined if exogenous expression of BST-2 reduces JUNV production in 293T cells. At 24 h p.t. of the BST-2 expressing plasmid, cells were infected under the same conditions (MOI = 0.1). Viral titers at 48 h p.i. showed a 3.04-fold reduction in JUNV production upon BST-2 expression, as compared to that in control cells (Fig. 2C). These results indicate a modest but statistically significant inhibitory effect of BST-2 on infectious JUNV production.

**Intracellular BST-2 expression is up-regulated upon JUNV infection and correlates with IFN levels**

In general, the innate immune response is triggered by viral infection. In the absence of an IFN antagonist, IFN induces the expression of a variety of ISGs, including BST-2 (25,45). To examine if JUNV infection affects BST-2 expression, the HeLa and A549 cells were infected with JUNV (Candid #1) at an MOI of 1.0, at 24 and 48 h p.i., the cell lysates were collected, and subjected to SDS-PAGE, followed by WB to analyze the expression levels of endogenous BST-2 compared to those in mock-infected cells. BST-2 expression was significantly increased at 48 h p.i. (by 1.8 times) in HeLa cells (Fig. 3A) and 17.2 times in A549 cells (Fig. 3B). We observed more intense BST-2 up-regulation in the case of A549 cells, partially because HeLa cells are known to express BST-2 endogenously without any stimulation (44). Hence, unlike mock-infected HeLa cells that showed higher BST-2 levels, A549 cells had very low background expression in mock-infected samples, which led to a higher induction of BST-2 at

48 h p.i.. This intense induction of BST-2 expression is unique to JUNV among the members of *Arenaviridae,* and has not been observed in LCMV infection (27). Based on the fact that BST-2 is an IFN-inducible protein (28), we next examined if BST-2 up-regulation correlates with IFN levels. The mRNA levels of *Ifn-β* were examined by quantitative real-time RT-PCR (qRT-PCR). A significant increase (53.8-fold) of *Ifn-β* mRNA was observed upon virus infection, compared to that in non-infected samples at 12 h p.i. in HeLa cells (Fig. 4A), which supports the observation of BST-2 upregulation upon IFN induction. We further ensured that the transcribed mRNA was translated into biologically active IFN-β protein. The production of IFN, induced as a result of JUNV infection, was examined by the growth inhibition of VSV in Vero76 cells. As shown in Fig. 4B, the treatment of Vero 76 cells with the culture supernatant from JUNV-infected cells significantly inhibited the growth of VSV compared to the controls at 12, 24, and 48 h p.i.. Our observation of the IFN response to JUNV is in agreement with previous report that described the induction of a type I IFN response to JUNV infection (12). Taken together, our results indicate a considerable increase in BST-2 expression upon JUNV infection, under the influence of the IFN response.

**Cell surface BST-2 expression is reduced upon JUNV infection**

We next investigated if the up-regulation of intracellular BST-2 level leads to the increase in BST-2 expression on the cell surface, where BST-2 tethers progeny virions. Fluorescence-activated cell sorting (FACS) analysis was performed to observe both intracellular as well as cell surface expression of BST-2 upon virus infection (MOI = 5.0). In agreement with the results from WB analysis (Fig. 3), intracellular BST-2 expression was increased at 48 h p.i. of JUNV (Candid #1) infection. We observed modest BST-2 up-regulation in HeLa cells (Fig. 5A left), compared to A549 cells, which showed a higher increase in BST-2 expression upon

infection (Fig. 5B left). In contrast, the cell surface expression of BST-2 was reduced in HeLa cells and was unchanged in A549 cells upon virus infection (Fig. 5 right panels). These results showed that JUNV infection up-regulates BST-2 expression by the induction of IFN, while cell surface expression is reduced by JUNV infection.

**JUNV NP counteracts the effect of BST-2 restriction on VLP production**

We next addressed if any of JUNV-encoded protein(s) could overcome BST-2 activity and rescue VLP production, as a reduction in cell surface BST-2 was observed upon JUNV infection. Previous research has shown that arenavirus NP and GP influence Z-mediated VLP production (46–49). Expression plasmid for JUNV NP, GPC or L protein was transfected into 293T cells with the Z expression plasmid in presence or absence of pCDNFL-hTeth. At 24 h p.t., VLPs were collected and analyzed as described in materials and methods. JUNV NP, but not GPC or L, rescued VLP production from BST-2 restriction (Fig. 6A and B). Consistent with the previous report (48), JUNV NP did not affect Z-mediated VLP production in 293T cells as compared to a sole expression of Z protein (Fig. 6C). However, in BST-2 expressing cells, significant recovery (13.4-fold increase) of VLP production by co-expression of NP was observed. To address whether JUNV NP could also counteract the function of endogenous BST-2, we analyzed Z-mediated VLP production in HeLa cells, which constitutively express endogenous BST-2. The JUNV Z expression plasmid was co-transfected into HeLa cells along with expression plasmid for NP, GPC or L. At 48 h p.t., VLPs were collected and analyzed, as described in materials and methods. As shown in Fig. 7, co-expression of NP, but not GPC or L, with Z protein led to the significant increase of VLP production (4.3-fold). Interestingly, co-expression of GPC with Z reduced VLP production in both 293T and HeLa cell lines (Figs. 6 and 7), which is consistent with the previous report for LASV (47). We also observed the co-

localization of JUNV NP and BST-2 in cells by a laser confocal microscopy (Fig. 8), which suggests a possible interaction between both proteins and supports the evidence that JUNV NP has the ability to partially rescue Z-mediated VLP production from BST-2 restriction.

To investigate whether JUNV NP can substitute for other viral BST-2 antagonist, such as HIV-1 Vpu and EBOV GP, we examined if JUNV NP can rescue the EBOV VP40-mediated VLP production from the BST-2 restriction. The expression plasmids for EBOV VP40 (pCEboZVP40) and BST-2 (pCDNFL-hTeth) were transfected into 293T cells with EBOV GP (pCEboZ-GP) or JNV NP (pC-Candid-NP) (Fig. 9A). EBOV VP40-mediated VLP productions were quantified (Fig. 9B). Consistent with the previous report (33), VLP production was significantly reduced by BST-2 expression. EBOV GP expression did not cause a significant enhancement of VP40-mediated VLP production, while EBOV GP expression could significantly recovered the reduction of VLP production by BST-2 expression (33). We also observed that JUNV NP can rescue EBOV VP40-mediated VLP production at the similar level to EBOV GP, suggesting that JUNV NP can also antagonize the restriction to other viruses by BST-2.

## DISCUSSION

Innate immune components are essential for the recognition of pathogen-associated molecular patterns in order to initiate an antiviral response, and to activate subsequent adaptive immunity (45). Host recognition of JUNV infection at early stages of infection mainly relies on two pathogen recognition receptors, the Toll-like receptor 2/6 heterodimer, which recognizes JUNV GP, and the cytoplasmic sensor RIG-I, which identifies viral dsRNA (12,50). Recognition of viral components leads to induction of the IFN response, which is the key mediator of the innate immunity to viral infections. On the other hand, it is reported that the arenavirus NP and Z proteins are antagonists of IFN production pathways (51,52). Clinical outcomes are distinct among arenaviruses. For instance, LASV infection shows immunosuppressive manifestations coupled with the lack of an IFN response (53,54). In contrast, JUNV infection is characterized by high levels of cytokines including IFN and tumor necrosis factor-alpha (55,56).

Previous studies have documented several ISGs, including RIG-I, MDA5, and Viperin, as innate immune factors with direct antiviral effect against JUNV (50,52,57). In this work, we expanded the list of ISGs involved in JUNV-host interaction. For the first time, we demonstrated that replication of the new world arenavirus, JUNV, is restricted by IFN-inducible protein, human BST-2. We have previously shown that LASV and LCMV Z protein-mediated VLP production is restricted by BST-2 (13,27). Similarly, we observed that the transient expression of BST-2 restricted JUNV Z-mediated VLP production (Fig. 1A and B), which is consistent with the previous report using MACV Z-mediated VLP production (26). Furthermore, TEM observations suggested that BST-2 tethered VLPs on the cell surface and restricted viral particle release (Fig. 1C). The same mechanism of action has been described for other enveloped viruses as well (23,58,59). The JUNV infection in BST-2 knocked-down HeLa cells (HeLa-TKD) and transiently over-expressed BST-2 in 293T cells resulted in a

modest increase and decrease in virus production, respectively (Fig. 2B and C). Interestingly, we observed that JUNV infection causes a remarkable up-regulation of BST-2 expression, which correlates with an increase in the type I IFN levels (Fig. 3 and 4). This finding has not been documented for any other arenaviruses, and could be explained on the basis of differences in the abilities of arenaviruses to counteract IFN production (60,61). Considering the fact that BST-2 also has immunoregulatory functions (62,63), it is tempting to ask whether BST-2 up-regulation is able to occur *in vivo* and what clinical implications this could have on the management of AHF patients.

Despite an increase in intracellular BST-2 levels, FACS analysis revealed the reduction of cell surface BST-2 expression upon JUNV infection. In order to exclude the possibility of cell line dependency on this observation, we performed experiments in two different cell lines (HeLa and A549) and observed that cell surface BST-2 reduced in HeLa cells, which suggests that JUNV is capable of restricting cell surface BST-2 (Fig. 5A). Furthermore, despite a more significant upregulation of intracellular BST-2 in A549 cells, we observed that cell surface BST-2 expression remained unchanged (Fig. 5B). These findings suggest that JUNV may also interfere with the trafficking of BST-2 proteins, which are induced and expressed upon infection, or that JUNV infection could induce the uptake of cell surface BST-2 into cytoplasm. Although JUNV infection caused a reduction of surface BST-2 (Fig. 5), intracellular BST-2 still caused a modest reduction in viral titers (Fig. 2B and 2C). The retention of viral particles in endosomes may explain the discrepancy in our observations. Altogether, these observations suggest the possibility that JUNV has an antagonistic activity against the antiviral action of BST-2. Experiments using individual viral proteins did not show any significant reduction of cell surface BST-2 expression (data not shown). However, JUNV NP expression recovered the reduction of Z-mediated VLP production by BST-2 (Fig. 6 and 7), indicating that NP possess the ability to antagonize the antiviral action of BST-2.

NP expression did not affect the expression levels of BST-2 in cells (Fig. 6 and 7). Therefore, it is unlikely that JUNV NP redirects BST-2 towards any degradative pathway, as well as HIV-1 Vpu (64,65). The expression of JUNV NP did not reduce the BST-2 expression on cell surface (data not shown). The antagonistic action of NP against BST-2 appears to be independent of the reduction of cell surface BST-2, which was observed in JUNV infected cells (Fig. 5). The JUNV NP may antagonize the BST-2 action by a mechanism other than the reduction of cell surface BST-2. In fact, EBOV GP has been reported to counteract BST-2 restriction in a manner that does not require the cell surface removal of BST-2 (33,36). Alternatively, it is possible that JUNV NP action is only a part of a more complex molecular mechanism leading to the reduction of cell surface BST-2. The JUNV infection may antagonize the antiviral action of BST-2 by multi-pathway, by multiple viral factors. The fact that JUNV NP can substitute for EBOV GP and rescue EBOV VP40-mediated VLP production suggests that the action mechanism of NP directly targets BST-2 protein. This is further supported by the co-localization of these two proteins in cells (Fig. 8 and 9). Therefore, it may be possible that JUNV NP relocates BST-2 away from membrane raft which are utilized for budding and release of enveloped viruses (66).

Prior to our finding that JUNV reduces the cell surface expression of BST-2, it was postulated that arenaviruses overcome the BST-2 restriction in an indirect manner (26). However, our results showed that JUNV has evolved to acquire an antagonistic mechanism against BST-2 function, and this is particularly plausible because of the drastic increase in intracellular BST-2 expression upon infection, which over time may have imposed an evolutionary selective pressure on JUNV. However, it is noteworthy that all experiments were conducted using the Candid #1 vaccine strain as a model, which has genetic variations compared to the highly pathogenic XJ13 and Romero strains of JUNV (67). While both strains, Romero and Candid #1, induce robust IFN production upon infection (12,68), the difference

between these two strains might influence the outcome, which we observed and reported in this study.

In conclusion, our results showed that the cell surface expression of BST-2 is reduced by JUNV infection, although JUNV infection induces IFN response and sequential BST-2 expression, and that the antiviral action of BST-2 against JUNV is partially antagonized by NP. Further analyses are required to understand the underlying molecular mechanisms.

## CONFLICT OF INTEREST

Authors declare that no conflict of interest exists.


## FUNDING INFORMATION

This work was supported by a grant-in-aid from the Japan Agency for Medical Research and Development (AMED) (grant numbers JP19fk0108072 and JP19fm0208101) for JY, and from the Japan Society for the Promotion of Science (JSPS) KAKENHI (grant number JP17K157902) for SU.

## ACKNOWLEDGMENTS

We thank Dr. J. C. de la Torre (The Scripps research Institute, California, USA) for providing JUNV Candid #1 strain and the plasmids coding JUNV proteins. We are grateful to all the members of the Department of Emerging Infectious Diseases and at the Institute of Tropical Medicine, Nagasaki University. We also thank the committee members and staff of the program for nurturing global leaders in Tropical and Emerging Communicable Diseases (TECD-Global leader) at the graduate school of biomedical sciences, Nagasaki university.

## REFERENCES


1. Maiztegui JI. Clinical and epidemiological patterns of Argentine haemorrhagic fever. Bull World Health Organ. 1975;52(4-5 6):567–75.

2. Enria DA, Briggiler AM, Sánchez Z. Treatment of Argentine hemorrhagic fever. Antiviral Res. 2008 Apr 1;78(1):132–9.

3. Grant A, Seregin A, Huang C, Kolokoltsova O, Brasier A, Peters C, et al. Junín Virus Pathogenesis and Virus Replication. Viruses. 2012 Oct 22;4(10):2317–39.

4. NIAID Emerging Infectious Diseases/Pathogens | NIH: National Institute of Allergy and Infectious Diseases [Internet]. [cited 2018 Nov 24]. Available from: https://www.niaid.nih.gov/research/emerging-infectious-diseases-pathogens

5. Urata S, Noda T, Kawaoka Y, Yokosawa H, Yasuda J. Cellular Factors Required for Lassa Virus Budding. J Virol. 2006 Apr;80(8):4191–5.

6. Fields BN. Fields Virology. Lippincott Williams & Wilkins; 2013. 2456 p.

7. Urata S, Yasuda J, de la Torre JC. The Z Protein of the New World Arenavirus Tacaribe Virus Has Bona Fide Budding Activity That Does Not Depend on Known Late Domain Motifs. J Virol. 2009 Dec 1;83(23):12651–5.

8. Strecker T, Eichler R, Meulen J t., Weissenhorn W, Dieter Klenk H, Garten W, et al. Lassa Virus Z Protein Is a Matrix Protein Sufficient for the Release of Virus-Like Particles. J Virol. 2003 Oct 1;77(19):10700–5.

9. Urata S, Yasuda J. Molecular Mechanism of Arenavirus Assembly and Budding. Viruses. 2012 Oct 10;4(10):2049–79.

10. Kranzusch PJ, Whelan SPJ. Arenavirus Z protein controls viral RNA synthesis by locking a polymerase–promoter complex. Proc Natl Acad Sci. 2011 Dec 6;108(49):19743–8.

11. Radoshitzky SR, Abraham J, Spiropoulou CF, Kuhn JH, Nguyen D, Li W, et al. Transferrin receptor 1 is a cellular receptor for New World haemorrhagic fever arenaviruses. Nature. 2007 Mar 1;446(7131):92–6.

12. Huang C, Kolokoltsova OA, Yun NE, Seregin AV, Poussard AL, Walker AG, et al. Junín virus infection activates the type I interferon pathway in a RIG-I-dependent manner. PLoS Negl Trop Dis. 2012;6(5):e1659.

13. Sakuma T, Noda T, Urata S, Kawaoka Y, Yasuda J. Inhibition of Lassa and Marburg Virus Production by Tetherin. J Virol. 2009 Mar;83(5):2382–5.

14. Fukuma A, Abe M, Morikawa Y, Miyazawa T, Yasuda J. Cloning and characterization of the antiviral activity of feline Tetherin/BST-2. PloS One. 2011 Mar 29;6(3):e18247.

15. Takeda E, Nakagawa S, Nakaya Y, Tanaka A, Miyazawa T, Yasuda J. Identification and functional analysis of three isoforms of bovine BST-2. PloS One. 2012;7(7):e41483.

16. Fukuma A, Yoshikawa R, Miyazawa T, Yasuda J. A new approach to establish a cell line with reduced risk of endogenous retroviruses. PloS One. 2013;8(4):e61530.

17. Abe M, Fukuma A, Yoshikawa R, Miyazawa T, Yasuda J. Inhibition of budding/release of porcine endogenous retrovirus. Microbiol Immunol. 2014 Aug;58(8):432–8.

18. Douglas JL, Gustin JK, Viswanathan K, Mansouri M, Moses AV, Früh K. The Great Escape: Viral Strategies to Counter BST-2/Tetherin. PLOS Pathog. 2010 May 13;6(5):e1000913.

19. Sauter D, Specht A, Kirchhoff F. Tetherin: Holding On and Letting Go. Cell. 2010 Apr 30;141(3):392–8.

20. Yasuda J. Ebolavirus Replication and Tetherin/BST-2. Front Microbiol [Internet]. 2012 Apr 2 [cited 2018 Nov 25];3. Available from: https://www.ncbi.nlm.nih.gov/pmc/articles/PMC3316994/

21. Ishikawa J, Kaisho T, Tomizawa H, Lee BO, Kobune Y, Inazawa J, et al. Molecular cloning and chromosomal mapping of a bone marrow stromal cell surface gene, BST2, that may be involved in pre-B-cell growth. Genomics. 1995 Apr 10;26(3):527–34.

22. Kupzig S, Korolchuk V, Rollason R, Sugden A, Wilde A, Banting G. Bst-2/HM1.24 is a raft-associated apical membrane protein with an unusual topology. Traffic Cph Den. 2003 Oct;4(10):694–709.

23. Perez-Caballero D, Zang T, Ebrahimi A, McNatt MW, Gregory DA, Johnson MC, et al. Tetherin inhibits HIV-1 release by directly tethering virions to cells. Cell. 2009 Oct 30;139(3):499–511.

24. Sakuma T, Sakurai A, Yasuda J. Dimerization of Tetherin Is Not Essential for Its Antiviral Activity against Lassa and Marburg Viruses. PLOS ONE. 2009 Sep 9;4(9):e6934.

25. Neil SJD, Zang T, Bieniasz PD. Tetherin inhibits retrovirus release and is antagonized by HIV-1 Vpu. Nature. 2008 Jan;451(7177):425–30.

26. Radoshitzky SR, Dong L, Chi X, Clester JC, Retterer C, Spurgers K, et al. Infectious Lassa virus, but not filoviruses, is restricted by BST-2/tetherin. J Virol. 2010 Oct;84(20):10569–80.

27. Urata S, Kenyon E, Nayak D, Cubitt B, Kurosaki Y, Yasuda J, et al. BST-2 controls T cell proliferation and exhaustion by shaping the early distribution of a persistent viral infection. PLOS Pathog. 2018 Jul 20;14(7):e1007172.

28. Neil SJD, Sandrin V, Sundquist WI, Bieniasz PD. An Interferon-α-Induced Tethering Mechanism Inhibits HIV-1 and Ebola Virus Particle Release but Is Counteracted by the HIV-1 Vpu Protein. Cell Host Microbe. 2007 Sep 13;2(3):193–203.

29. Van Damme N, Goff D, Katsura C, Jorgenson RL, Mitchell R, Johnson MC, et al. The interferon-induced protein BST-2 restricts HIV-1 release and is downregulated from the cell surface by the viral Vpu protein. Cell Host Microbe. 2008 Apr 17;3(4):245–52.

30. Yamada E, Nakaoka S, Klein L, Reith E, Langer S, Hopfensperger K, et al. Human-Specific Adaptations in Vpu Conferring Anti-tetherin Activity Are Critical for Efficient Early HIV-1 Replication In Vivo. Cell Host Microbe. 2018 Jan 10;23(1):110-120.e7.

31. Douglas JL, Viswanathan K, McCarroll MN, Gustin JK, Früh K, Moses AV. Vpu Directs the Degradation of the Human Immunodeficiency Virus Restriction Factor BST-2/Tetherin via a βTrCP-Dependent Mechanism. J Virol. 2009 Aug 15;83(16):7931–47.

32. Le Tortorec A, Neil SJD. Antagonism to and intracellular sequestration of human tetherin by the human immunodeficiency virus type 2 envelope glycoprotein. J Virol. 2009 Nov;83(22):11966–78.

33. Kaletsky RL, Francica JR, Agrawal-Gamse C, Bates P. Tetherin-mediated restriction of filovirus budding is antagonized by the Ebola glycoprotein. Proc Natl Acad Sci U S A. 2009 Feb 24;106(8):2886–91.

34. Hu S, Yin L, Mei S, Li J, Xu F, Sun H, et al. BST-2 restricts IAV release and is countered by the viral M2 protein. Biochem J. 2017 20;474(5):715–30.

35. Mansouri M, Viswanathan K, Douglas JL, Hines J, Gustin J, Moses AV, et al. Molecular mechanism of BST2/tetherin downregulation by K5/MIR2 of Kaposi's sarcoma-associated herpesvirus. J Virol. 2009 Oct;83(19):9672–81.

36. Lopez LA, Yang SJ, Hauser H, Exline CM, Haworth KG, Oldenburg J, et al. Ebola Virus Glycoprotein Counteracts BST-2/Tetherin Restriction in a Sequence-Independent Manner That Does Not Require Tetherin Surface Removal. J Virol. 2010 Jul 15;84(14):7243–55.

37. Urata S, Uno Y, Kurosaki Y, Yasuda J. The cholesterol, fatty acid and triglyceride synthesis pathways regulated by site 1 protease (S1P) are required for efficient replication of severe fever with thrombocytopenia syndrome virus. Biochem Biophys Res Commun. 2018 Sep 5;503(2):631–6.

38. Yasuda J, Nakao M, Kawaoka Y, Shida H. Nedd4 Regulates Egress of Ebola Virus-Like Particles from Host Cells. J Virol. 2003 Sep 15;77(18):9987–92.

39. Ueda MT, Kurosaki Y, Izumi T, Nakano Y, Oloniniyi OK, Yasuda J, et al. Functional mutations in spike glycoprotein of Zaire ebolavirus associated with an increase in infection efficiency. Genes Cells. 2017 Feb;22(2):148–59.

40. Emonet SF, Seregin AV, Yun NE, Poussard AL, Walker AG, de la Torre JC, et al. Rescue from Cloned cDNAs and In Vivo Characterization of Recombinant Pathogenic Romero and Live-Attenuated Candid #1 Strains of Junin Virus, the Causative Agent of Argentine Hemorrhagic Fever Disease. J Virol. 2011 Feb 15;85(4):1473–83.

41. Watanabe K, Ishikawa T, Otaki H, Mizuta S, Hamada T, Nakagaki T, et al. Structure-based drug discovery for combating influenza virus by targeting the PA–PB1 interaction. Sci Rep [Internet]. 2017 Dec [cited 2018 Nov 26];7(1). Available from: http://www.nature.com/articles/s41598-017-10021-w

42. Roles of YIGL sequence of Ebola virus VP40 on genome replication and particle production | Microbiology Society [Internet]. [cited 2020 Feb 11]. Available from: https://www.microbiologyresearch.org/content/journal/jgv/10.1099/jgv.0.001286

43. Loureiro ME, Zorzetto-Fernandes AL, Radoshitzky S, Chi X, Dallari S, Marooki N, et al. DDX3 suppresses type I interferons and favors viral replication during Arenavirus infection. PLOS Pathog. 2018 Jul 12;14(7):e1007125.

44. Miyagi E, Andrew AJ, Kao S, Strebel K. Vpu enhances HIV-1 virus release in the absence of Bst-2 cell surface down-modulation and intracellular depletion. Proc Natl Acad Sci. 2009 Feb 24;106(8):2868–73.

45. Iwasaki A. A Virological View of Innate Immune Recognition. Annu Rev Microbiol. 2012;66(1):177–96.

46. Shtanko O, Imai M, Goto H, Lukashevich IS, Neumann G, Watanabe T, et al. A Role for the C Terminus of Mopeia Virus Nucleoprotein in Its Incorporation into Z Protein-Induced Virus-Like Particles. J Virol. 2010 May 15;84(10):5415–22.

47. Urata S, Yasuda J. Cis- and cell-type-dependent trans-requirements for Lassa virus-like particle production. J Gen Virol. 2015 Jul 1;96(7):1626–35.

48. Groseth A, Wolff S, Strecker T, Hoenen T, Becker S. Efficient Budding of the Tacaribe Virus Matrix Protein Z Requires the Nucleoprotein. J Virol. 2010 Apr 1;84(7):3603–11.

49. Casabona JC, Levingston Macleod JM, Loureiro ME, Gomez GA, Lopez N. The RING Domain and the L79 Residue of Z Protein Are Involved in both the Rescue of Nucleocapsids and the Incorporation of Glycoproteins into Infectious Chimeric Arenavirus-Like Particles. J Virol. 2009 Jul 15;83(14):7029–39.

50. Cuevas CD, Ross SR. Toll-Like Receptor 2-Mediated Innate Immune Responses against Junín Virus in Mice Lead to Antiviral Adaptive Immune Responses during Systemic Infection and Do Not Affect Viral Replication in the Brain. J Virol. 2014 Jul 15;88(14):7703–14.

51. Martínez-Sobrido L, Giannakas P, Cubitt B, García-Sastre A, Torre JC de la. Differential Inhibition of Type I Interferon Induction by Arenavirus Nucleoproteins. J Virol. 2007 Nov 15;81(22):12696–703.

52. Fan L, Briese T, Lipkin WI. Z Proteins of New World Arenaviruses Bind RIG-I and Interfere with Type I Interferon Induction. J Virol. 2010 Feb 15;84(4):1785–91.

53. Huang C, Kolokoltsova OA, Yun NE, Seregin AV, Ronca S, Koma T, et al. Highly Pathogenic New World and Old World Human Arenaviruses Induce Distinct Interferon Responses in Human Cells. J Virol. 2015 Jul;89(14):7079–88.

54. Russier M, Pannetier D, Baize S. Immune Responses and Lassa Virus Infection. Viruses. 2012 Nov;4(11):2766–85.

55. Levis SC, Saavedra MC, Ceccoli C, Falcoff E, Feuillade MR, Enria DAM, et al. Endogenous Interferon in Argentine Hemorrhagic Fever. J Infect Dis. 1984 Mar 1;149(3):428–33.

584 56. Marta RF, Montero VS, Hack CE, Sturk A, Maiztegui JI, Molinas FC. Proinflammatory
585 cytokines and elastase-alpha-1-antitrypsin in Argentine hemorrhagic fever. Am J Trop
586 Med Hyg. 1999 Jan 1;60(1):85–9.

587 57. Peña Cárcamo JR, Morell ML, Vázquez CA, Vatansever S, Upadhyay AS, Överby AK,
588 et al. The interplay between viperin antiviral activity, lipid droplets and Junín
589 mammarenavirus multiplication. Virology. 2018 Jan;514:216–29.

590 58. Hammonds J, Wang J-J, Yi H, Spearman P. Immunoelectron Microscopic Evidence for
591 Tetherin/BST2 as the Physical Bridge between HIV-1 Virions and the Plasma
592 Membrane. PLoS Pathog [Internet]. 2010 Feb 5 [cited 2019 May 7];6(2). Available
593 from: https://www.ncbi.nlm.nih.gov/pmc/articles/PMC2816691/

594 59. Mangeat B, Cavagliotti L, Lehmann M, Gers-Huber G, Kaur I, Thomas Y, et al.
595 Influenza Virus Partially Counteracts Restriction Imposed by Tetherin/BST-2. J Biol
596 Chem. 2012 Jun 22;287(26):22015–29.

597 60. Borrow P, Martínez-Sobrido L, De la Torre JC. Inhibition of the Type I Interferon
598 Antiviral Response During Arenavirus Infection. Viruses. 2010 Nov;2(11):2443–80.

599 61. Pythoud C, Rothenberger S, Martínez-Sobrido L, de la Torre JC, Kunz S. Lymphocytic
600 Choriomeningitis Virus Differentially Affects the Virus-Induced Type I Interferon
601 Response and Mitochondrial Apoptosis Mediated by RIG-I/MAVS. J Virol. 2015
602 Jun;89(12):6240–50.

603 62. Loschko J, Schlitzer A, Dudziak D, Drexler I, Sandholzer N, Bourquin C, et al. Antigen
604 delivery to plasmacytoid dendritic cells via BST2 induces protective T cell-mediated
605 immunity. J Immunol Baltim Md 1950. 2011 Jun 15;186(12):6718–25.

606 63. Li SX, Barrett BS, Heilman KJ, Messer RJ, Liberatore RA, Bieniasz PD, et al. Tetherin
607 promotes the innate and adaptive cell-mediated immune response against retrovirus
608 infection in vivo. J Immunol Baltim Md 1950. 2014 Jul 1;193(1):306–16.

609 64. Gupta RK, Hué S, Schaller T, Verschoor E, Pillay D, Towers GJ. Mutation of a Single
610 Residue Renders Human Tetherin Resistant to HIV-1 Vpu-Mediated Depletion. Hope
611 TJ, editor. PLoS Pathog. 2009 May 22;5(5):e1000443.

612 65. Dubé M, Paquay C, Roy BB, Bego MG, Mercier J, Cohen ÉA. HIV-1 Vpu Antagonizes
613 BST-2 by Interfering Mainly with the Trafficking of Newly Synthesized BST-2 to the
614 Cell Surface. Traffic. 2011 Dec;12(12):1714–29.

615 66. Chazal N, Gerlier D. Virus Entry, Assembly, Budding, and Membrane Rafts. Microbiol
616 Mol Biol Rev. 2003 Jun 1;67(2):226–37.

617 67. Stephan BI, Lozano ME, Goñi SE. Watching Every Step of the Way: Junín Virus
618 Attenuation Markers in the Vaccine Lineage. Curr Genomics. 2013 Nov;14(7):415–24.

619 68. Huang C, Kolokoltsova OA, Mateer EJ, Koma T, Paessler S. Highly Pathogenic New
620 World Arenavirus Infection Activates the Pattern Recognition Receptor Protein Kinase
621 R without Attenuating Virus Replication in Human Cells. J Virol [Internet]. 2017 Sep
622 27 [cited 2019 Jun 14];91(20). Available from:
623 https://www.ncbi.nlm.nih.gov/pmc/articles/PMC5625494/

## FIGURE LEGENDS

**Figure 1.** BST-2 restricts JUNV Z-mediated particle release. (A) Western blot analysis (Anti-FLAG; upper and middle panel for the detection of JUNV Z and BST-2, respectively. Anti-β-Actin; loading control) of VLPs produced from 293T cells transfected with pC-JUNV Z-FLAG and either control plasmid or pCDNFL-hTeth, and cell-associated proteins. (B) Quantified results of six independent experiments. The bar indicates standard deviation (**: $p < 0.01$). (C) Electron microscopy evidence for retention and clustering of JUNV Z-mediated VLPs, under the expression of BST-2. The 293T cells were transfected with control plasmids (i) or with plasmids expressing JUNV Z (ii), or co-transfected with plasmids for JUNV Z and BST-2 (iii, iv). At 24 h p.t., ultrathin sections were prepared for electron microscopy analysis. Arrows indicate JUNV Z-mediated VLPs, tethered on the cell membrane. Bar; 200 nm.

**Figure 2.** BST-2 modestly restricts JUNV (Candid #1) propagation. (A) Detection of endogenous BST-2 expression in HeLa-pLKO and HeLa-TKD cells using antibody against BST-2. (B) JUNV production from HeLa-TKD and HeLa-pLKO cells. Both cells were infected with JUNV at an MOI = 0.1, and the culture media was collected at 24 and 48 h p.i.. Viral titers in the supernatant were determined by the plaque assay (n = 6). (C) Effect of exogenous BST-2 expression on JUNV propagation. Control plasmid or pCDNFL-hTeth was transfected into 293T cells and infected with JUNV (Candid #1) at an MOI of 0.1. At 48 h p.i., viral titers were determined by plaque assay (n = 6). The graph represents results of six independent experiments. The bars indicate standard deviation (*: $p < 0.05$; **: $p < 0.01$).

**Figure 3.** Endogenous BST-2 expression was induced upon JUNV (Candid #1) infection. HeLa cells (A) and A549 cells (B) were infected with JUNV (Candid #1) at an MOI = 0.1. The BST-2 expression level was analyzed at 24 and 48 h p.i. by western blotting (n = 6, *: $p < 0.05$).

**Figure 4.** Type-I interferon expression is induced in response to JUNV (Candid #1) infection. (A) *Ifn-β* mRNA transcripts of JUNV (Candid #1)-infected and non-infected HeLa cells were quantified by quantitative RT-PCR (RT-qPCR) at 12 h p.i. (n = 6). Results were normalized against transcription levels of *Gapdh* (*Ifn-β/Gapdh*) using the ΔΔCt calculation method. (B) Bioactive interferon levels in the supernatant of mock or JUNV (Candid #1)-infected HeLa cells (12, 24, and 48 h p.i.) were determined by the reduction of VSV cytopathic effects in Vero 76 cells.

**Figure 5.** JUNV (Candid #1) infection interfered with surface BST-2 expression. (A) HeLa and (B) A549 cells were infected with JUNV (Candid #1) at an MOI of 5.0. At 48 h p.i., cells were fixed and permeabilized (intracellular, left) or not (surface, right), and stained with PE-conjugated anti-BST-2 antibody or isotype control antibody, for FACS analysis.

**Figure 6.** BST-2 mediated restriction of VLP production is counteracted by JUNV NP protein. (A) 293T cells were transfected with JUNV-Z-FLAG, with or without FLAG-BST-2, JUNV NP, GPC, L expressing and/or empty vectors. At 24 h p.t., VLPs were detected by western blotting (n = 4). (B) Expression of Z protein was quantified and normalized to cellular expression levels (Z-mediated VLP/cell-associated Z). (C) Promotion of VLP production by JUNV NP in BST-2 expressing cells. The bars indicate standard deviation (**: $p < 0.01$).

669 **Figure 7.** Z-mediated VLP production is promoted by JUNV NP in HeLa cells. (A and B)
670 HeLa cells were transfected with pC-JUNV-Z-FLAG with or without JUNV NP, GPC, L
671 expression vector and/or empty vector. At 24 h p.t., VLPs were analyzed as described in figure
672 6. The bars indicate standard deviation (**: $p < 0.01$).

673

674 **Figure 8.** JUNV NP co-localizes with BST-2. In A549 cells transfected with pC-JUNVNP-
675 FLAG plasmid, endogenous BST-2 expression was induced by IFN-β and staining was
676 performed as described in materials and methods. The white arrows indicate co-localization of
677 JUNV NP and BST-2. Bar; 5 μm.

678

679 **Figure 9.** JUNV NP antagonizes the BST-2-induced restriction on Ebola virus (EBOV) VP40-
680 mediated VLP production. (A) 293T cells were transfected with pCEboZ VP40 along with
681 pCEboZ-GP or pC-Candid-NP-FLAG in the presence or absence of BST-2 expression. At 24
682 h p.t., VLPs were detected by western blotting (n = 4). (B) Intensities of VP40 protein were
683 quantified and the VLP productions were normalized to the cellular expression levels of VP40
684 (VLP-associated VP40/cell-associated VP40). The bars indicate standard deviation (**: $p <$
685 0.01).

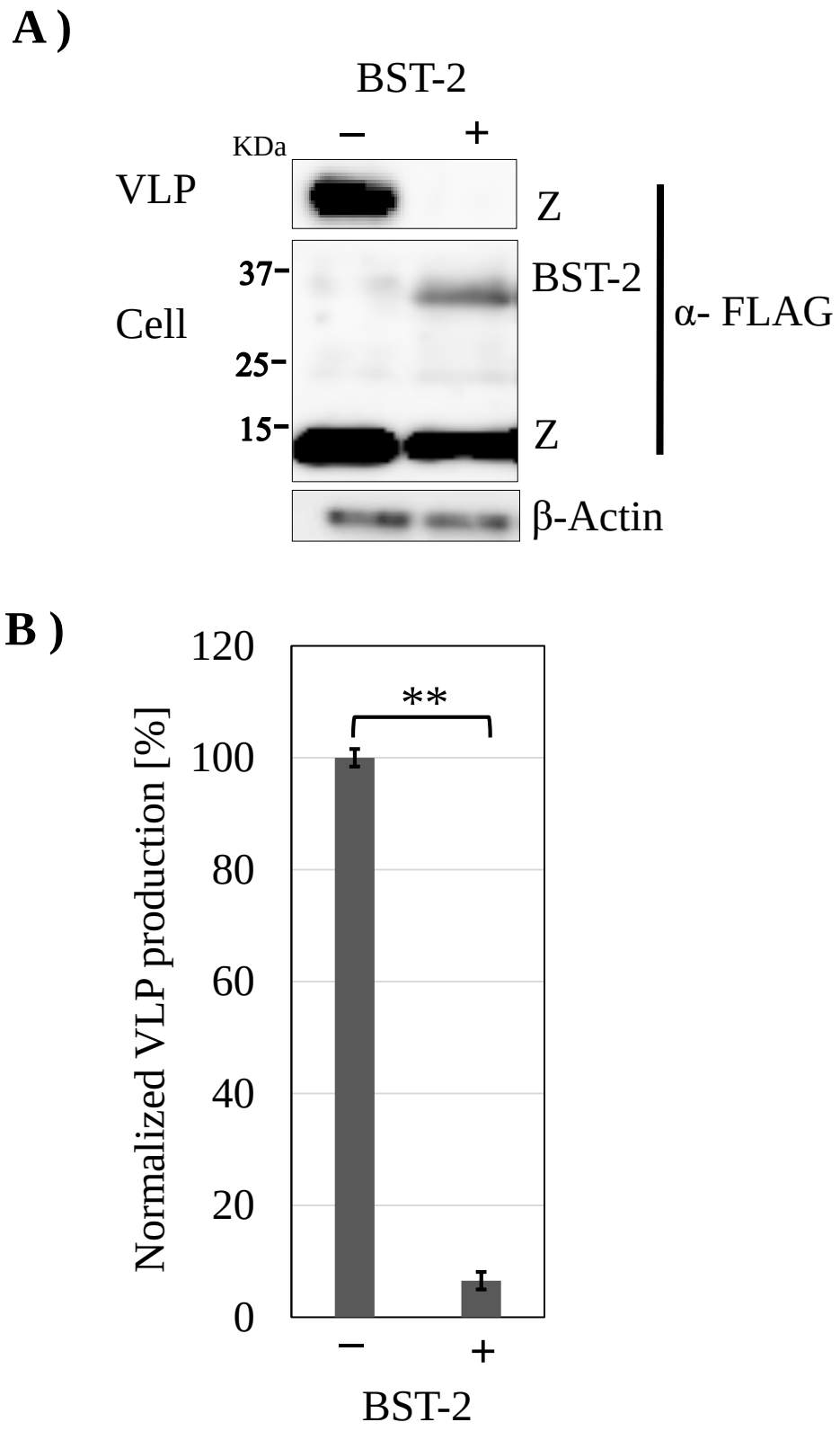


**Figure 1 A and B. Zadeh *et al.***

C )

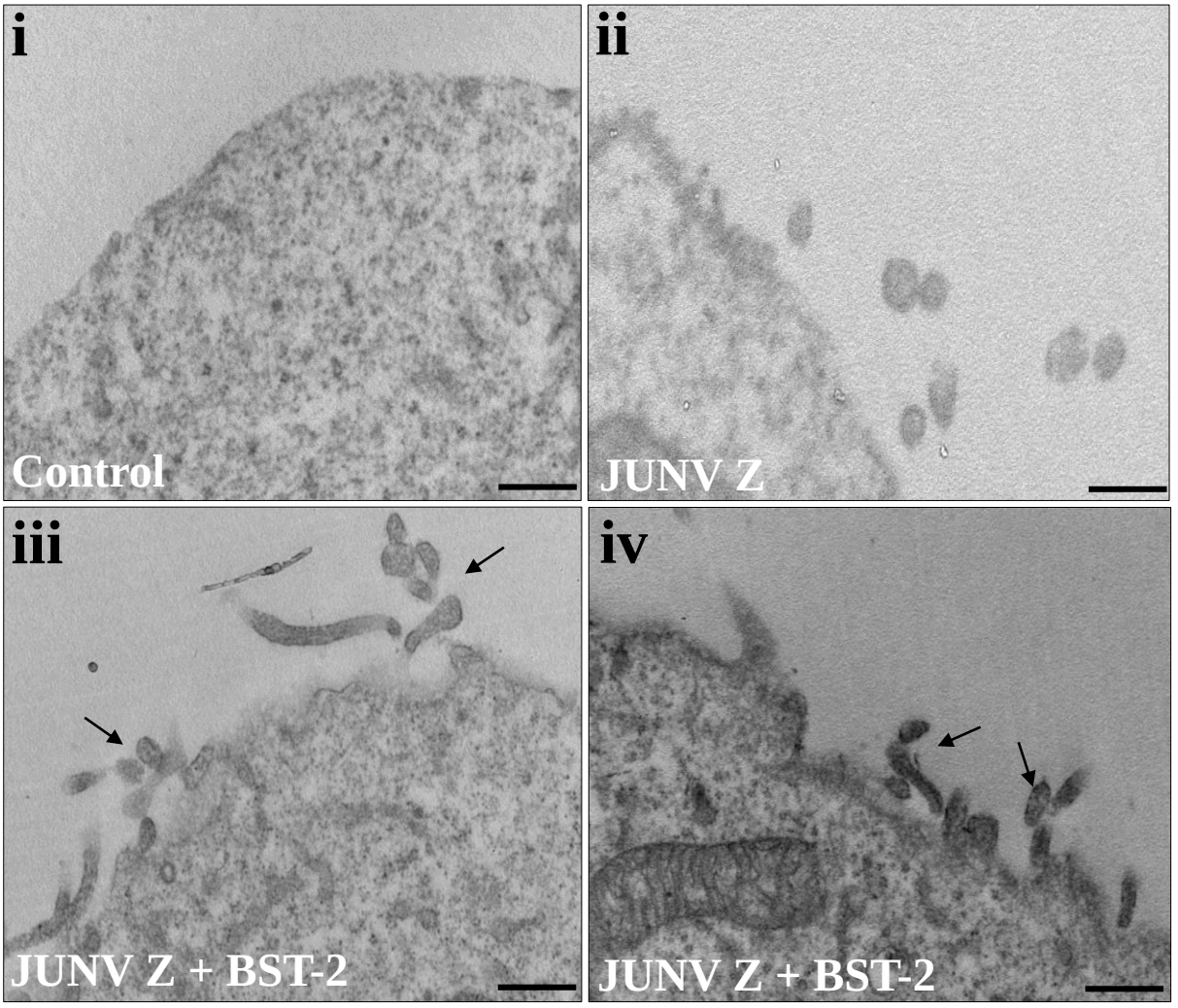


**Figure 1 C. Zadeh *et al.***

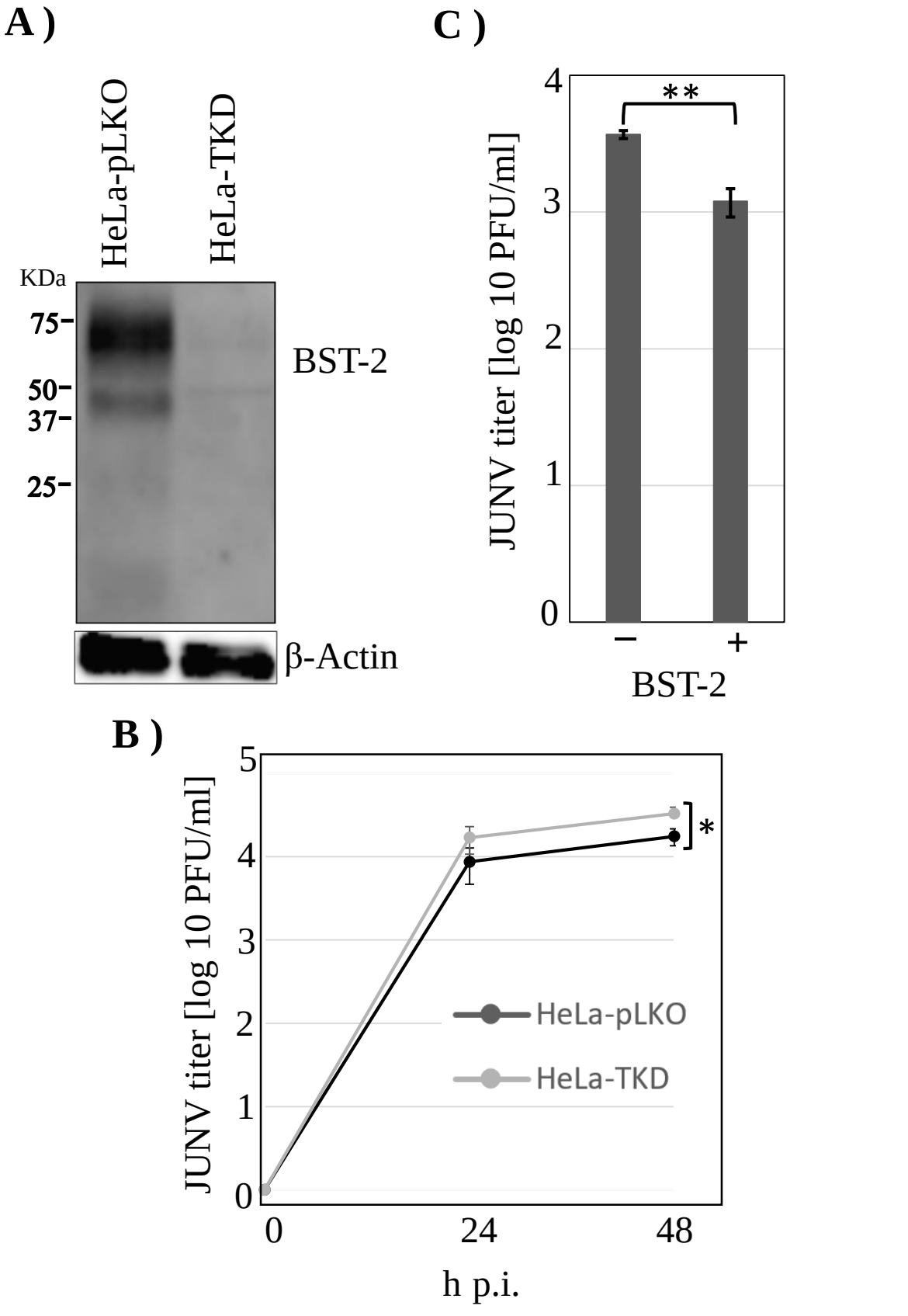


**Figure 2. Zadeh *et al.***

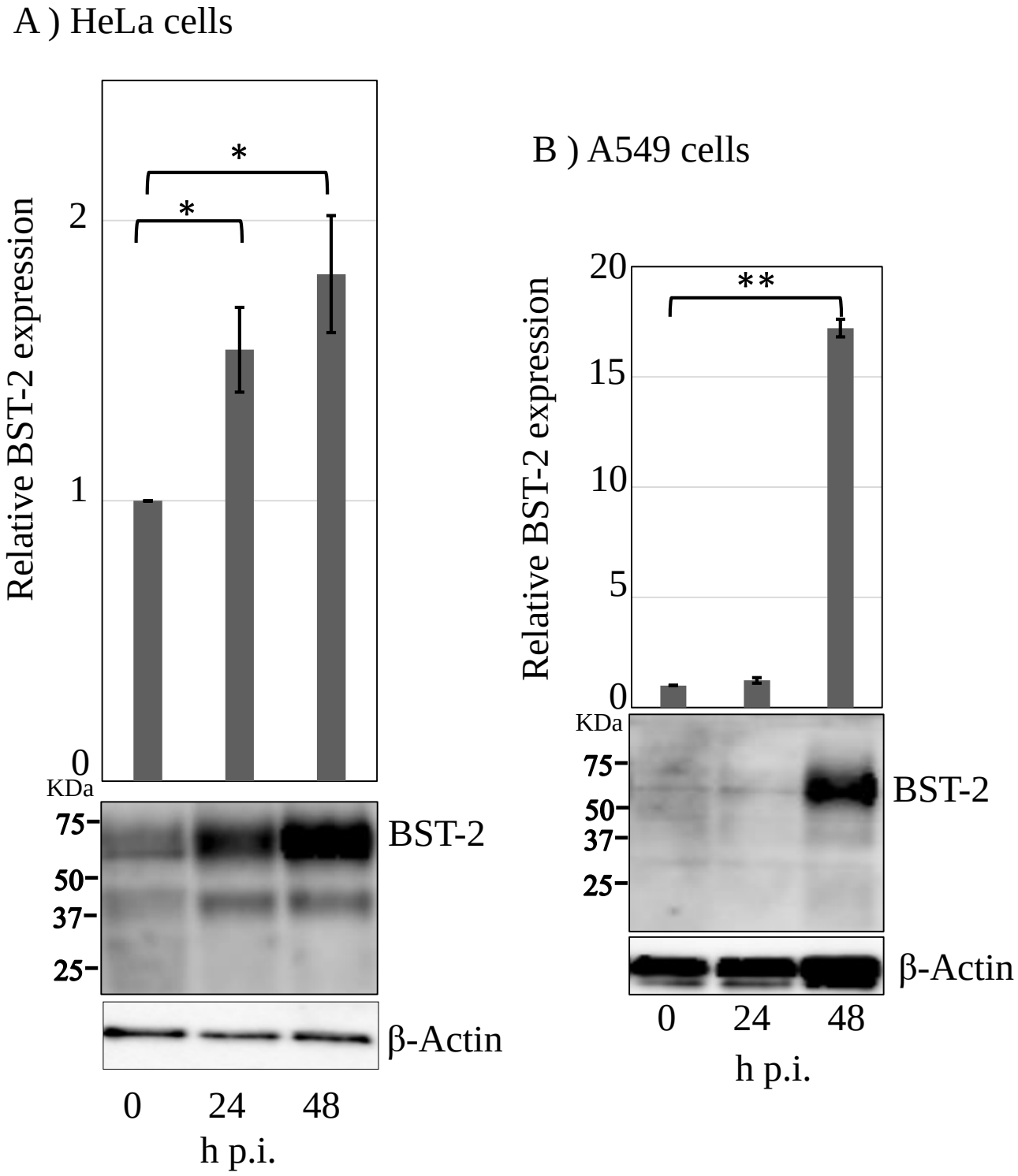


**Figure 3. Zadeh *et al.***

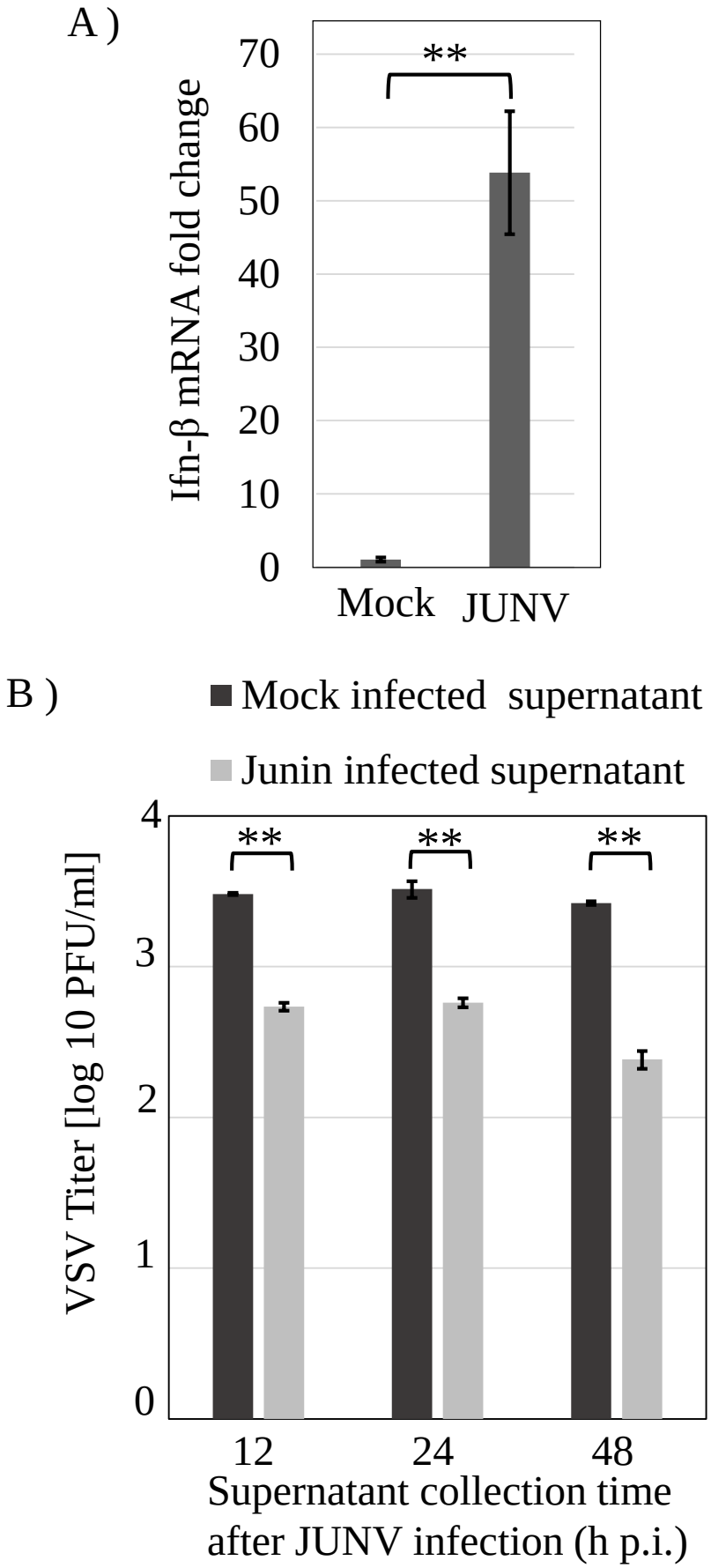


**Figure 4. Zadeh *et al.***

A ) HeLa cells

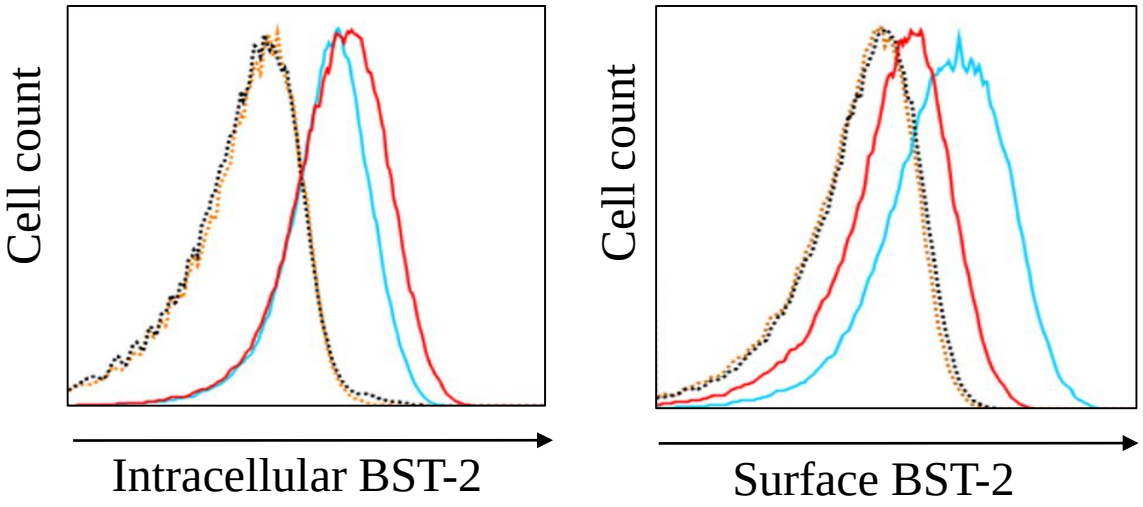


B ) A549 cells

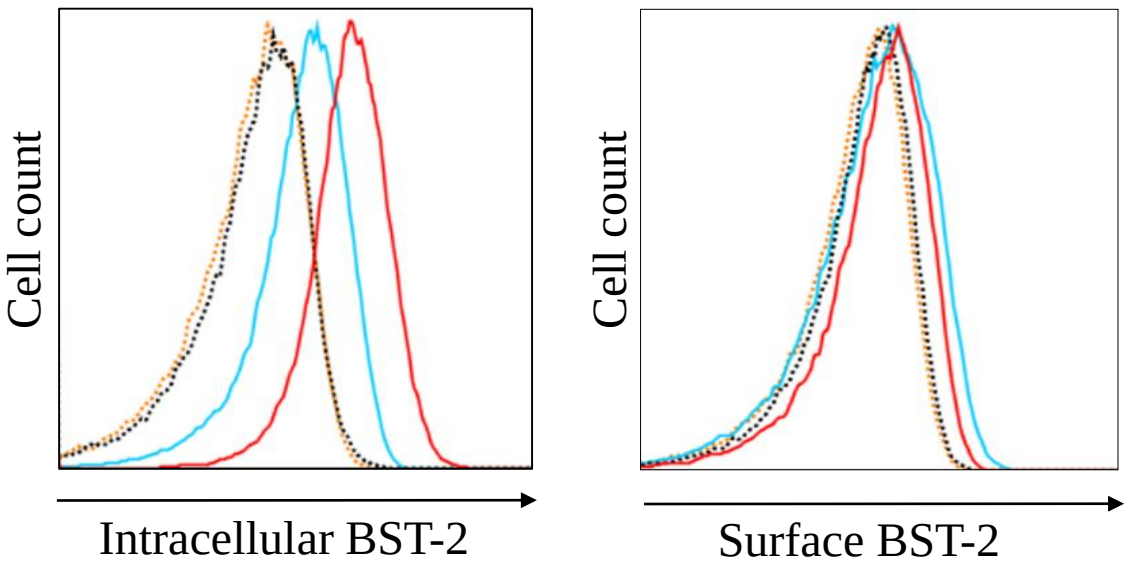


**<u>Dots: Isotype control</u>**
Orange: Mock-infected
Black: Infected

**<u>Line: anti-hBST-2 Ab</u>**
Blue: Mock-infected
Red: Infected

**Figure 5. Zadeh *et al.***

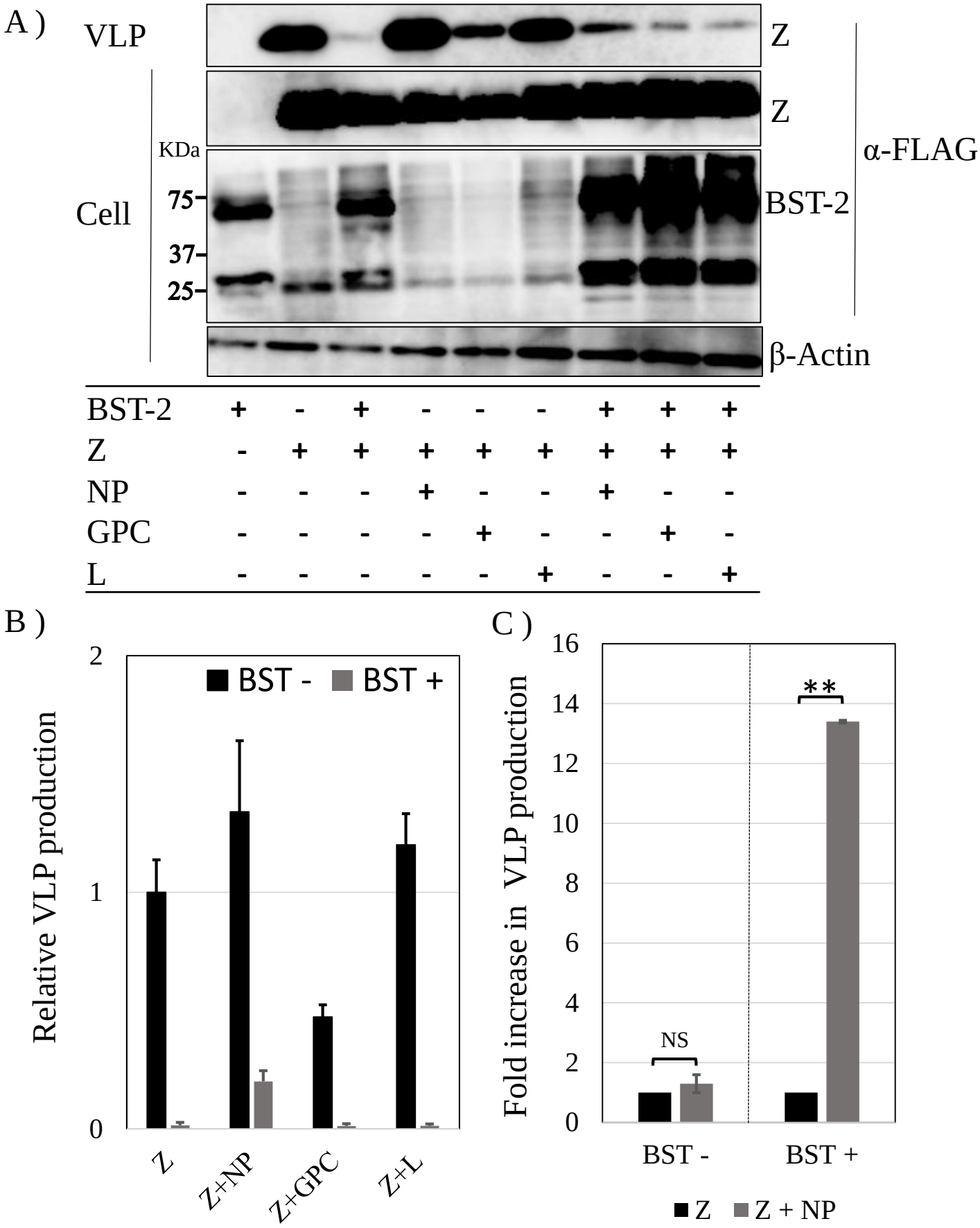




**Figure 6. Zadeh *et al.***

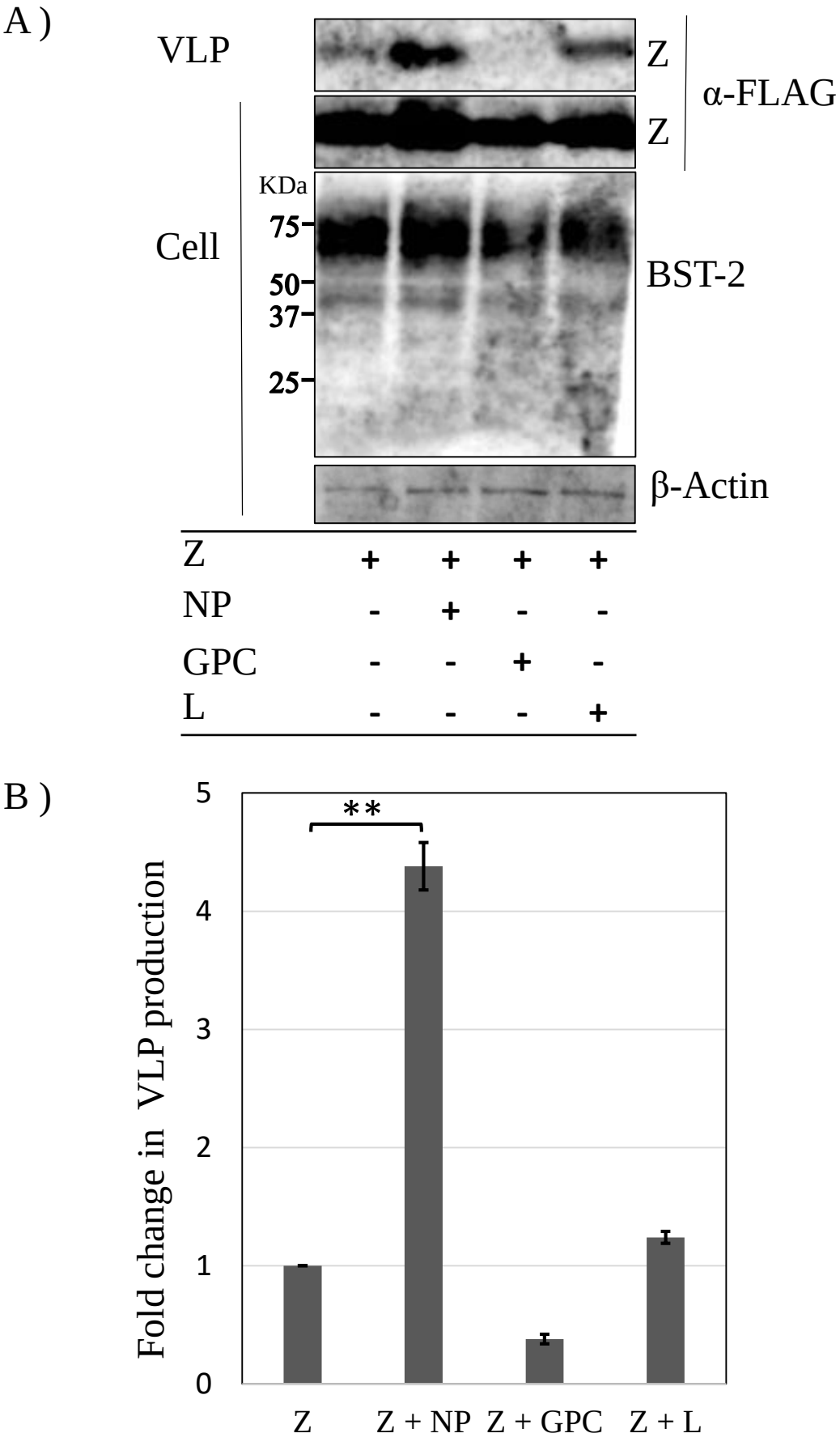




**Figure 7. Zadeh *et al.***

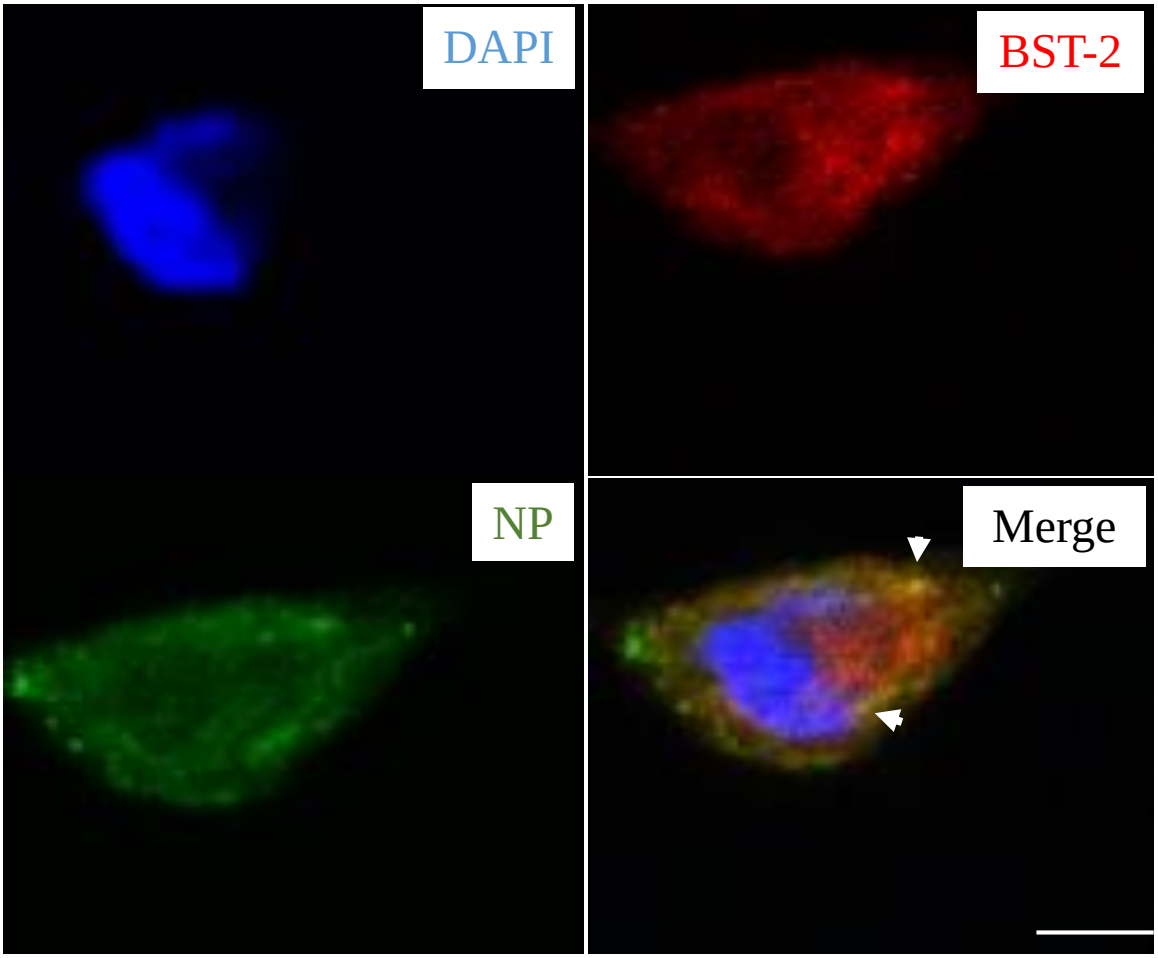




**Figure 8. Zadeh *et al.***

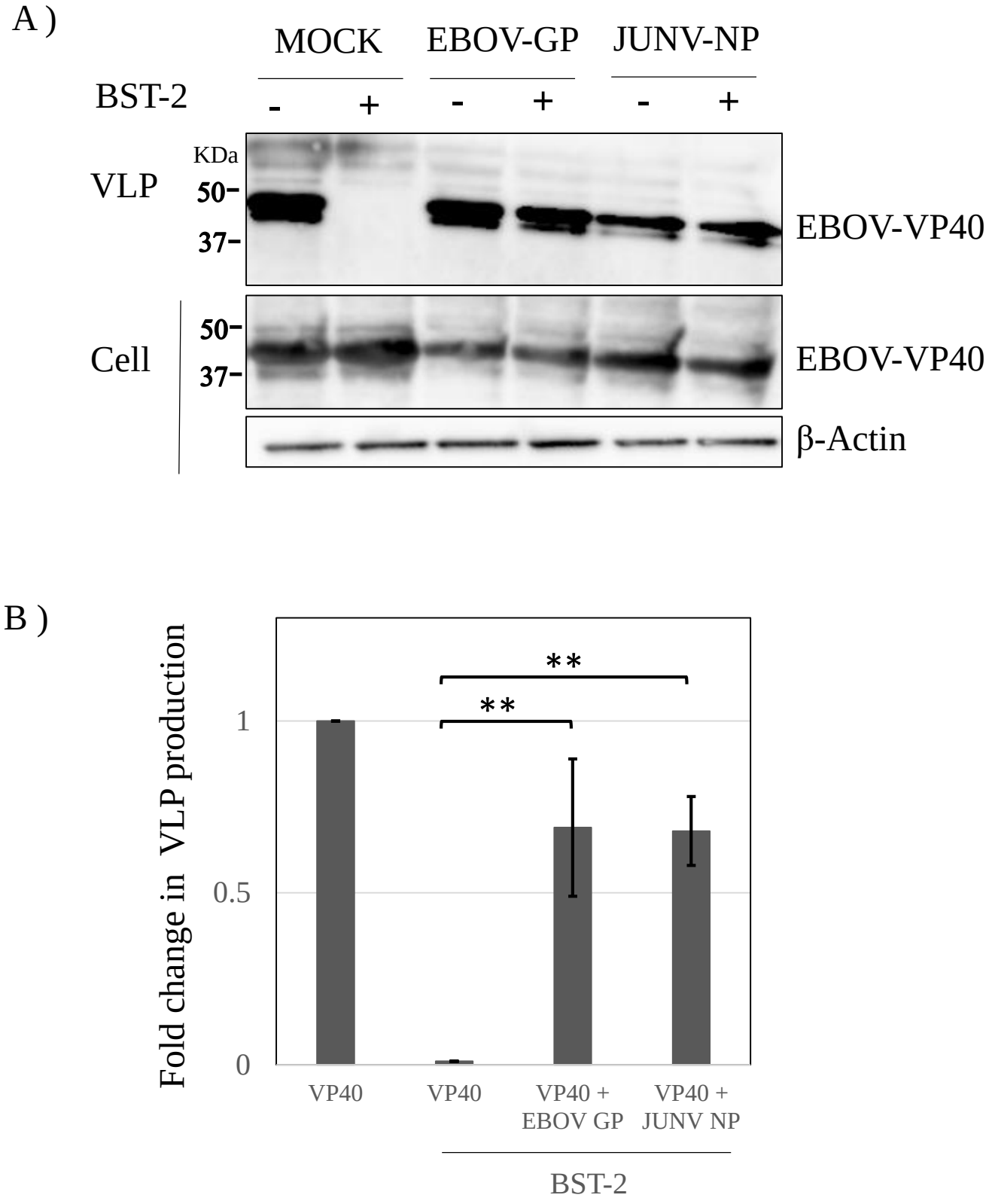




**Figure 9. Zadeh *et al.***